Renormalization of Molecular Electronic Levels at Metal-Molecule Interfaces

J. B. Neaton,[1] Mark S. Hybertsen,[2] and Steven G. Louie[1,3]

[1]*The Molecular Foundry, Materials Sciences Division, Lawrence Berkeley National Laboratory, Berkeley, California 94720, USA*
[2]*Department of Applied Physics and Applied Mathematics and Center for Electron Transport in Molecular Nanostructures, Columbia University, New York, New York 10027, USA*
[3]*Department of Physics, University of California, Berkeley, California 94720, USA*

(Received 18 June 2006; published 22 November 2006)

The electronic structure of benzene on graphite (0001) is computed using the *GW* approximation for the electron self-energy. The benzene quasiparticle energy gap is predicted to be 7.2 eV on graphite, substantially reduced from its calculated gas-phase value of 10.5 eV. This decrease is caused by a change in electronic correlation energy, an effect completely absent from the corresponding Kohn-Sham gap. For weakly coupled molecules, this correlation energy change can be described as a surface polarization effect. A classical image potential model illustrates the impact for other conjugated molecules on graphite.

DOI: 10.1103/PhysRevLett.97.216405 PACS numbers: 85.65.+h, 31.70.Dk, 71.10.−w, 73.20.−r

There is renewed interest in using organic molecules as components in nanoscale electronic and optoelectronic devices [1,2], and thus a critical need has emerged for improved knowledge and control of charge transport phenomena in these systems [3]. Understanding transport across the interface between the active organic layer and the metallic electrode has proved particularly challenging, especially in the single-molecule limit. Fundamentally, charge transport is controlled in such systems by the electronic coupling of frontier molecular orbitals to extended states in the electrode, and the energetic position of these orbitals relative to the contact Fermi level. Several recent measurements of organic thin films, self-assembled monolayers (SAMs), and single-molecule junctions have emphasized the important role of Coulomb interactions between the added hole or electron in the frontier orbitals and the metal substrate [4–11]. However, most theoretical calculations of transport through organic molecules have continued to rely on some implementation of density functional theory (DFT) or semiempirical one-particle Hamiltonians [3]. The limitations of DFT for describing excited-state energies are well known [12], and implications for a DFT-based theory for nanoscale conductance have been recently discussed [13].

When a molecule is brought in contact with a metal, several physical effects will influence its ionization level (highest occupied molecular orbital, HOMO) and affinity level (lowest unoccupied molecular orbital, LUMO). First, the self-consistent interaction between molecule and surface will rearrange the electron density and modify the alignment of frontier orbital energies. Second, electronic coupling to extended states in the metal will further shift orbital energies and broaden discrete molecular levels into resonances. Finally, the Coulomb interaction between the added hole or electron associated with the ionization or affinity level will result in a polarization of the metal substrate. This additional correlation energy further stabilizes the added hole or electron, reducing the gap between affinity and ionization levels as illustrated in Fig. 1. An accurate DFT-based approach should correctly capture the first effect [14], although the use of DFT to calculate the width of resonances is under debate [13]. Importantly, however, the surface polarization response, as we show here, is completely absent from frontier orbital energies computed in DFT.

In this Letter, we compute the electronic excited states for an example of a weakly coupled system, an aromatic molecule (benzene) physisorbed on the graphite (0001) surface. Electronic correlations are included directly within a first-principles many-electron Green function approach [15]. The electron self-energy is calculated from first principles within the *GW* approximation (GWA) [16] using a methodology [17] that has proved accurate for a wide range of systems [18]. While more generally including dynamical electronic correlation, the GWA is well known to include static, long-range image potential effects for an electron near an interface [19]. Using this approach, we predict a strong renormalization of the electronic gap of the benzene system (relative to its molecular gas-phase value) when it is physisorbed on a graphite (0001) surface.

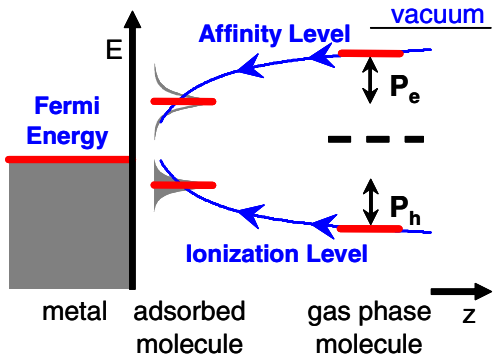

FIG. 1 (color online). Schematic energy level diagram indicating polarization shifts in the frontier energy levels (ionization and affinity) of a molecule upon adsorption on a metal surface.

The change in gap on adsorption can be quite generally understood as a polarization effect. An image potential model is used to illustrate trends for other aromatic molecules weakly coupled to a metal surface.

Equilibrium geometries of molecular benzene in the gas phase, condensed in a bulk crystalline phase, and physisorbed on graphite (0001) are determined using DFT within the local density approximation (LDA). Norm-conserving pseudopotentials [20] are used with a plane-wave basis (80 Ry cutoff) for structural relaxations. The surface is modeled with a 3×3 supercell containing 4 layers of graphite, a single benzene molecule, and the equivalent of 7 layers of vacuum. The theoretical in-plane bulk lattice parameter is used ($a = 2.45$ Å, $c = 6.62$ Å). In the most stable site for adsorption, benzene rests flat on the surface centered on a threefold site 3.25 Å above a substrate carbon atom, in agreement with a previous study [21]. For comparison, benzene is also considered in an upright position, centered above a hollow site with its closest hydrogen atom 2.21 Å from the surface. Solid crystalline benzene has an orthorhombic unit cell containing four molecules (Pbca); the atomic positions within the unit cell are optimized keeping the lattice parameters a, b, and c fixed to their experimental values of 7.44, 9.55, and 6.92 Å, respectively [22]. The gas phase is modeled using a cubic supercell ($a = 13.22$ Å). For each system, matrix elements of the self-energy operator are evaluated using a 50 Ry energy cutoff for the electronic wave functions, a 6 Ry cutoff for the momentum-space dielectric matrix, and a 2.9 Ry cutoff for the sum over virtual states. This choice of parameters results in quasiparticle energy gaps converged within ~0.2 eV.

The electron addition and removal energies of a benzene molecule in the gas phase, calculated in the present GW approach, result in a HOMO-LUMO (quasiparticle) gap of 10.51 eV. This value agrees well with an independent GW calculation [23], total energy difference calculations based on DFT [24,25], and experiment [26]. By contrast, the Kohn-Sham gap (within LDA) is 5.16 eV, substantially smaller. The electronic structure of benzene on the graphite (0001) surface along the Γ-K' direction is shown in Fig. 2. Comparing the surface-projected band structures (shaded regions) in Fig. 2(a) and 2(b), the quasiparticle bandwidth increases by about 15% relative to LDA, in agreement with previous works [27,28]. The bold horizontal lines interpolate between the benzene HOMO and LUMO states computed at Γ and K'; the filled circles at these high-symmetry points indicate states with significant weight on the molecule. For physisorbed benzene, the Kohn-Sham (LDA) gap is 5.05 eV throughout the zone, unchanged from the corresponding LDA gas-phase value. Relative to the LDA value, the quasiparticle gap of the molecule flat on the graphite surface is much *larger*, 7.35 eV. However, the predicted quasiparticle gap is substantially *smaller* than the gas-phase value of 10.51 eV.

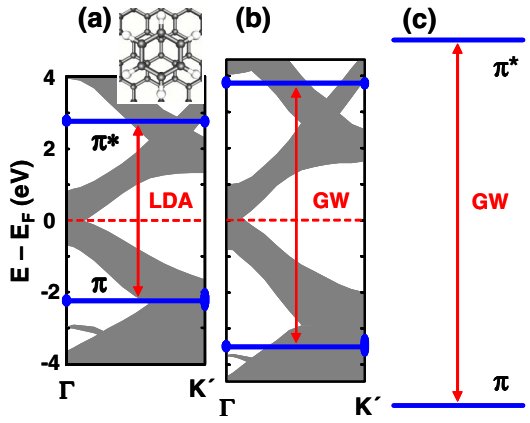

FIG. 2 (color online). Calculated frontier orbital energy levels (heavy blue lines) with the indicated energy gap (red arrows) for benzene adsorbed flat on the graphite surface, plotted against the projected surface band structure of graphite: (a) DFT (LDA) energies, (b) GW quasiparticle energies, (c) GW quasiparticle energies of benzene in the gas phase. Inset in (a) shows a model of the adsorption geometry.

Table I summarizes the calculated HOMO-LUMO gaps of benzene in four environments. Remarkably, the LDA gaps are identical in all cases. In contrast, the GW self-energy corrections exhibit noticeable variation. To understand this, we analyze the self-energy change relative to the gas phase. The change $\Delta\Sigma$ for each frontier level is decomposed into Coulomb-hole ($\Delta\Sigma_{\mathrm{CH}}$), screened-exchange ($\Delta\Sigma_{\mathrm{SX}}$), and bare exchange or Fock ($\Delta\Sigma_X$) contributions. We find that $\Delta\Sigma_{\mathrm{CH}}$ is nearly equal for the occupied and empty frontier states, and that $\Delta\Sigma_X$ is quite small (0.1–0.2 eV). Interestingly, the screened-exchange term is responsible for most of the difference: for the HOMO, we observe $\Delta\Sigma_{\mathrm{SX}} \sim -2\Delta\Sigma_{\mathrm{CH}}$, while for the LUMO $\Delta\Sigma_{\mathrm{SX}} \sim 0$. Put together, the change in correlation energy ($\Delta\Sigma_{\mathrm{Corr}} = \Delta\Sigma_{\mathrm{CH}} + \Delta\Sigma_{\mathrm{SX}}$) reported in Table I turns out to be nearly symmetric between the ionization and affinity levels for the benzene in each environment studied. A similar result was

TABLE I. Benzene HOMO-LUMO gaps in the gas phase, crystal phase, and adsorbed on the graphite surface (flat and perpendicular). First and second lines are Kohn-Sham (LDA) and quasiparticle (GW) gaps. (For the crystal, we average over the π and π^* manifolds.) Third and fourth lines are calculated changes in correlation energy for the HOMO and LUMO, relative to the gas phase, determined from the full GW calculations and from an image potential model. Energies are in eV.

	Gas phase	Flat graphite	Perp graphite	Crystal phase
ΔE_{gap} (LDA)	5.16	5.05	5.11	5.07
ΔE_{gap} (GW)	10.51	7.35	8.10	7.91
$\Delta\Sigma_{\mathrm{Corr}}$		1.45, −1.51	1.18, −1.17	1.16, −1.15
$\Delta\Sigma_{\mathrm{Corr}}$ (Model)		1.50, −1.43	0.97, −0.96	

obtained from a previous derivation of the image potential for an electron near a metal surface [19].

Since the benzene frontier orbitals are weakly coupled and well separated from the substrate Fermi energy, we may now proceed with a general analysis of the self-energy operator that is broadly applicable to molecular adsorbates on a range of different metal substrates. For such systems the overlap of the molecular frontier orbitals with the substrate is small, and the self-energy correction upon adsorption will depend only on the change in the screened Coulomb interaction W, i.e.,

$$\Delta\Sigma_{\mathrm{SX}}(\mathbf{r},\mathbf{r}';E)=\sum_{j}^{\mathrm{occ}}\phi_j(\mathbf{r})\phi_j^*(\mathbf{r}')\Delta W(\mathbf{r},\mathbf{r}';E-E_j), \quad (1)$$

where ϕ_j are molecular wave functions and E_j their eigenvalues. A corresponding expression exists for the Coulomb-hole term. For sufficiently large metal-molecule separations, ΔW is smooth and slowly varying over the spatial extent of the molecular orbitals, and only the self-term contributes to the matrix elements of Eq. (1). Then the change in correlation energy from the surface can be reduced to

$$\begin{aligned}\Delta E_{\mathrm{HOMO}} &= \langle\phi_{\mathrm{HOMO}}|\Delta\Sigma_{\mathrm{SX}}+\Delta\Sigma_{\mathrm{CH}}|\phi_{\mathrm{HOMO}}\rangle \\ &\approxeq 2P_{\mathrm{HOMO}}-P_{\mathrm{HOMO}} \\ &= P_{\mathrm{HOMO}} \end{aligned} \quad (2)$$

and

$$\begin{aligned}\Delta E_{\mathrm{LUMO}} &= \langle\phi_{\mathrm{LUMO}}|\Delta\Sigma_{\mathrm{SX}}+\Delta\Sigma_{\mathrm{CH}}|\phi_{\mathrm{LUMO}}\rangle \\ &\approxeq 0-P_{\mathrm{LUMO}} \\ &= -P_{\mathrm{LUMO}}, \end{aligned} \quad (3)$$

where P is the static polarization integral

$$P_j=-\frac{1}{2}\iint d\mathbf{r}d\mathbf{r}'\phi_j(\mathbf{r})\phi_j^*(\mathbf{r}')\Delta W(\mathbf{r},\mathbf{r}')\phi_j(\mathbf{r}')\phi_j^*(\mathbf{r}). \quad (4)$$

For benzene on graphite, the full GW calculations indicate that dynamical effects make a negligible contribution to $\Delta\Sigma_{\mathrm{Corr}}$, and that the self-term accounts for more than 90% of $\Delta\Sigma_{\mathrm{Corr}}$, supporting the simplified picture of Eqs. (2)–(4).

Additional simplification is achieved if an image potential model suffices for $\Delta W(\mathbf{r},\mathbf{r})$. In Fig. 3, we plot the screening potential, $\Delta W(\mathbf{r},\mathbf{r})=\Delta V_{\mathrm{scr}}(\mathbf{r},\mathbf{r})$, where $V_{\mathrm{scr}}(\mathbf{r},\mathbf{r})$ results from the screening response to the added electron (or hole) [17]. The difference $\Delta V_{\mathrm{scr}}(\mathbf{r},\mathbf{r})$ for the adsorbed and isolated molecules is also compared with an image model, $1/4|z-z_0|$, where the image plane position z_0 is determined separately [29] to be 1 Å beyond the outer surface plane for our graphite slab. From Fig. 3, the model performs well over the spatial range of the molecular orbital. Using z_0 given above and the isolated frontier orbitals, P_{HOMO} and P_{LUMO} are calculated for benzene in

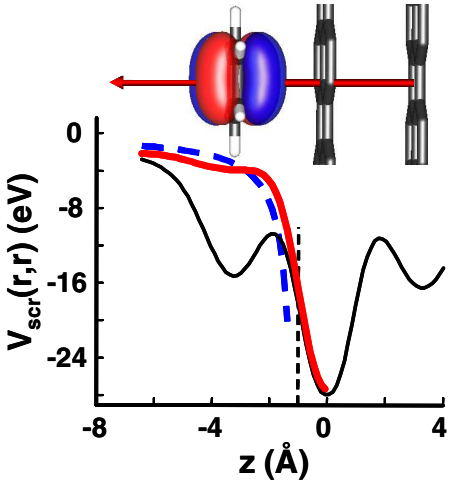

FIG. 3 (color online). Static screening potential, $V_{\mathrm{scr}}(\mathbf{r},\mathbf{r})$, plotted along a line through benzene adsorbed flat on graphite. Thin, solid (black) curve is the total $V_{\mathrm{scr}}(\mathbf{r},\mathbf{r})$ for the metal-molecule system; the thick, solid (red) curve is $\Delta V_{\mathrm{scr}}(\mathbf{r},\mathbf{r})$, the change upon adsorption; the heavy, dashed (blue) curve is the image potential model relative to the image plane (light, vertical dashed line). Inset: physical model, scaled to the axis of the plot, including an isosurface plot of a frontier benzene π orbital.

flat and perpendicular geometries using the image potential model. As shown in Table I, the model is quite accurate for the flat case and captures most of the effect for the perpendicular case (within 0.2 eV). The simple image potential model neglects the internal screening response of the molecule to the polarization of the metal surface. While small for a flat molecule oriented parallel to a surface, an appreciable molecular polarizability perpendicular to the metal surface would increase P_j.

For molecular resonances well separated from the metal Fermi energy, the image model for $\Delta\Sigma$ should be broadly applicable, provided that the substrate-dependent image plane is properly calculated. In Table II, we use the image model to predict the renormalized gaps for members of the acene series and coronene adsorbed flat on graphite. For the larger molecules in the series, the change in gap is dramatic, e.g., the pentacene gap is predicted to diminish by nearly a factor of 2 on a graphite surface.

The role of geometry and morphology on changes in polarization energy in organic systems can be subtle [30], but the impact has been measured for organic films on metal substrates using photoemission and inverse photoemission [6]. Adsorbate frontier orbital energies can also be probed by STM, provided the HOMO-LUMO gap is small enough to access the resonant tunneling regime [7,31]. From Table II, tetracene and pentacene are within typical measurement range (±2.5 V), while anthracene and coronene are marginal. In a recent study of pentacene adsorbed on ultrathin NaCl on Cu(111) [11], gaps of 3.3, 4.1, and 4.4 eV are observed for NaCl thicknesses of one, two, and three monolayers, respectively. Our predicted

TABLE II. For selected molecules, measured gas-phase ioniziation energies and electron affinities [26] are combined with an image model for polarization energies to predict adsorbate HOMO-LUMO gaps for molecules flat on graphite (all in eV).

Molecule	Experiment IP	Experiment EA	Gas-phase gap	P_{HOMO}	P_{LUMO}	Adsorbate gap
Naphthalene	8.14	−0.20	8.34	1.41	1.39	5.54
Anthracene	7.44	0.53	6.91	1.32	1.30	4.29
Tetracene	6.97	0.88	6.09	1.24	1.23	3.62
Pentacene	6.63	1.39	5.24	1.18	1.18	2.88
Coronene	7.29	0.47	6.82	1.19	1.17	4.46

value of 2.9 eV for direct adsorption on the graphite surface fits well with this progression.

In conclusion, we find that the correlation contribution to the frontier molecular orbital energies depends sensitively on environment. In the examples studied here, the change in correlation energy is dominated by a polarization effect. The impact of electrode surface polarization on spectroscopic measurements must be carefully assessed for each metal-molecule system. For organic films or SAMs, the polarization contribution from neighboring molecules can also be quite significant. For molecular systems where the frontier orbitals have stronger electronic coupling and the resultant resonances overlap with the metal Fermi energy, the role of dynamical charge transfer is expected to be considerable, and future investigations must address the nature of additional contributions to the self-energy in this case.

We thank Professor G. W. Flynn and Dr. C. D. Spataru for useful discussions. Portions of this work were performed at the Molecular Foundry, which is supported by the Office of Science, Office of Basic Energy Sciences, of the US Department of Energy under Contract No. DE-AC02-05CH11231. This work was partially supported by the Nanoscale Science and Engineering Initiative of the NSF under Grant No. CHE-0117752, the New York State Office of Science, Technology, and Academic Research (NYSTAR). This work was also partially supported by the NSF under Grant No. DMR04-39768. Computational resources were provided by NERSC and NPACI.

[1] C. D. Dimitrakopoulos and P. R. L. Malenfant, Adv. Mater. **14**, 99 (2002).
[2] C. Joachim, J. K. Gimzewski, and A. Aviram, Nature (London) **408**, 541 (2000).
[3] A. Nitzan and M. A. Ratner, Science **300**, 1384 (2003).
[4] A. Kahn, N. Koch, and W. Y. Gao, J. Polym. Sci., B Polym. Phys. **41**, 2529 (2003).
[5] S. Kubatkin *et al.*, Nature (London) **425**, 698 (2003).
[6] E. V. Tsiper *et al.*, Chem. Phys. Lett. **360**, 47 (2002).
[7] X. H. Lu *et al.*, Phys. Rev. B **70**, 115418 (2004).
[8] S. C. Veenstra *et al.*, Appl. Phys. A **75**, 661 (2002).
[9] C. D. Zangmeister *et al.*, J. Phys. Chem. B **108**, 16 187 (2004).
[10] X. Y. Zhu, J. Phys. Chem. B **108**, 8778 (2004).
[11] J. Repp *et al.*, Phys. Rev. Lett. **94**, 026803 (2005).
[12] R. O. Jones and O. Gunnarsson, Rev. Mod. Phys. **61**, 689 (1989).
[13] M. Koentopp, K. Burke, and F. Evers, Phys. Rev. B **73**, 121403(R) (2006).
[14] G. Heimel *et al.*, Phys. Rev. Lett. **96**, 196806 (2006).
[15] L. Hedin and S. Lundquist, in *Solid State Physics*, edited by F. Seitz and D. Turnbull (Academic, New York, 1969), p. 1.
[16] L. Hedin, Phys. Rev. **139**, A796 (1965).
[17] M. S. Hybertsen and S. G. Louie, Phys. Rev. B **34**, 5390 (1986).
[18] W. G. Aulbur, L. Jonsson, and J. W. Wilkins, in *Solid State Physics*, edited by H. Ehrenreich (Academic, New York, 1999), p. 1.
[19] J. C. Inkson, J. Phys. C **6**, 1350 (1973).
[20] N. Troullier and J. L. Martins, Phys. Rev. B **43**, 1993 (1991).
[21] A. J. Fisher and P. E. Blochl, Phys. Rev. Lett. **70**, 3263 (1993).
[22] G. E. Bacon, N. A. Curry, and S. A. Wilson, Proc. R. Soc. A **279**, 98 (1964).
[23] M. L. Tiago and J. R. Chelikowsky, Solid State Commun. **136**, 333 (2005).
[24] J. C. Rienstra-Kiracofe *et al.*, J. Phys. Chem. A **105**, 524 (2001).
[25] L. A. Curtiss *et al.*, J. Chem. Phys. **109**, 42 (1998).
[26] S. L. Murov, I. Carmichael, and G. L. Hug, *Handbook of Photochemistry* (M. Dekker, New York, 1993).
[27] C. Heske *et al.*, Phys. Rev. B **59**, 4680 (1999).
[28] S. Y. Zhou *et al.*, Phys. Rev. B **71**, 161403(R) (2005).
[29] S. C. Lam and R. J. Needs, J. Phys. Condens. Matter **5**, 2101 (1993).
[30] E. V. Tsiper and Z. G. Soos, Phys. Rev. B **68**, 085301 (2003).
[31] M. Lackinger *et al.*, J. Phys. Chem. B **108**, 2279 (2004).